Seismic Vulnerability Analysis of Bridges in Mountainous States

Matt Hardman
Thomas Wilson
Suren Chen

Department of Civil and Environmental Engineering
Colorado State University
Fort Collins, CO 80523

September 2013

ACKNOWLEDGEMENT

The funds for this study were provided by the United States Department of Transportation to the Mountain Plains Consortium (MPC). Matching funds were provided by Colorado State University.

DISCLAIMER

ABSTRACT

Depending on the location, highway bridges can often support considerable amounts of traffic. Due to the limitations on current earthquake forecasting techniques, a normal amount of traffic will also typically remain on a bridge when an earthquake occurs. In addition to traffic, scour effects are also a potential hazard to bridge piers that may simultaneously impact the structural integrity of the bridge together with seismic loads. Although a few studies investigating the combined effect of extreme and service loads have been conducted on long-span bridges or in high-seismic zones, the studies on typical short- and medium-span bridges in low and moderate seismic zones are rare. A general dynamic simulation methodology is introduced to study the combined realistic service and extreme loads on short- and medium-span bridges. Following the introduction of the methodology, a numerical study investigating the seismic performance of a typical highway bridge in mountainous states is carried out. The bridge is subjected to different combinations of traffic, seismic, and scour and the effects on the structural performance of the bridge are investigated. The bridge, including both superstructure and substructure, is modeled in detail using SAP2000 to accommodate the goals of this study. The traffic load is considered through dynamic interaction analysis of vehicles in the simulated stochastic traffic flow. Through studying the bridge performance under various combined extreme and service loads, findings are made about controlling cases for different bridge responses and the validity of the traditional superposition approach with consideration to load combinations is also discussed. As the initial effort studied the bridge performance under multiple service and extreme loads, this study sheds some light on more comprehensive studies for the future.

TABLE OF CONTENTS

LIST OF FIGURES

LIST OF TABLES

1. INTRODUCTION AND LITERATURE REVIEW

1.1 BACKGROUND

In recent years, growing concerns over seismic design requirements of bridges in both high and moderate seismic regions have created new areas of study. Much of the movement of the design philosophy is heading away from force-based designs, which had previously been the standard in earthquake engineering. Performance-based design and assessment is the newer philosophy coming out of the research efforts over the past few years. Such a design philosophy is aimed at creating more reliable structures through conducting optimal designs, especially in extreme events. In addition to designing against a single hazard, a relatively new field gaining more interest is to design a modern bridge in an extreme event where other realistic service and extreme conditions may also exist. Mountainous states are not traditional earthquake-intensive area,s and no high standard of seismic design of bridges is typically adopted. As a result, little information is available about the bridge performance subjected to earthquake as well as other service and extreme loads. In order to better understand the seismic designs of bridges in the context of multiple hazards, a comprehensive literature review of the related topics is given in the following.

1.2 LITERATURE REVIEW

The intent of the following section is to encompass necessary information as background for the following study. The topics covered in the literature review section include: bridge seismic hazard, multiple hazard resistance, load interactions of traffic and bridges, and interactions of bridge seismic and scour.

1.2.1 Bridge Seismic Hazard

In the United States, the primary natural hazards being designed for in the major structural design codes are: earthquakes, floods, and high winds. Earthquakes are possibly the most difficult natural hazard to be designed for due to the lack of warning, rarity in frequency, and extreme consequences (FEMA 2004). Despite new advancements in the field of seismology, it is still difficult to predict the magnitude, location, and time of occurrence of any particular earthquake. The general characterization of the magnitudes and the frequency of a region, however, can be made based on geological setting and historical records. Some areas have been found to be more vulnerable to larger or less frequent earthquakes, while others may suffer from more frequent mild or moderate earthquakes. In structural design codes, seismic hazard maps provide information on the relative seismic exposure by assigning a hazard coefficient that is based on the probability of experiencing an earthquake and its relative magnitude. This coefficient determines the necessary design requirements needed to be met through the code design approach.

The need for the continued improvement on the resistance of bridges to earthquakes is also due to their unique importance in society as compared to other structures. Bridges are categorized as lifelines in inventories of the national infrastructure and assets. Critical bridges are necessary to help facilitate rescues, rebuilding, and other emergency services in the aftermath of a seismic event. Many studies have been conducted on assessing and improving the post-earthquake functionality of bridges. Part of this study, in line with these previous efforts, is to more

realistically assess the safety and serviceability of a critical bridge by considering the interaction with other extreme loads as well as normal service loads.

1.2.2 Multiple Hazard Resistance Concept

The design of structures for multiple hazards is a recent development in the world of engineering. Recently a lot of attention has been given to the development of a procedure for the design of structures to multiple hazards. The goal of such a procedure is to achieve safer and more economical designs for structures than those achieved using the conventional envelope method of design. One of the main driving forces behind this growing interest is that hazard maps clearly demonstrate most of the United States is vulnerable to at least one of the three main natural hazards: earthquakes, floods, and high winds. Another reason is the inconsistencies in current code on how different hazards affect structures, as well as how they are designed (FEMA 2004). The need for designing against multiple hazards calls for an integrated approach to design structures in the United States.

Utilizing an integrated approach in designs is very critical for those critical bridges subjected to multiple hazards, while being pivotal to local traffic at the same time. Dramatic progress has also been made on computer-based simulation technology allowing for carrying out complex structural analysis with simultaneous loads, including both extreme and service loads at the same time. As a result, a simple superposition of the bridge performance under individual loads, as adopted in most existing studies, may not give accurate prediction of bridges subjected to multiple loads (Chen and Wu 2010). The result of superposition may cause inconsistencies in design: this may stem from an underestimation of load interaction, or designing for a superimposed critical scenario leading to overdesign. Such an issue further develops the need for a truly integrated design approach for structures subjected to multiple hazards.

Moreover, another major problem in the design of structures for multiple hazards is in the lack of risk consistency. The lack of risk consistency stems from the use of different design philosophies currently being utilized for different hazards in the ASCE 07-05 Standard (Crosti et al. 2011). The future designs need to have risk levels that are the same among different structures in different locations based on the probabilities of exceedance from hazard maps. The work by Crosti et al. (2011) shows that a structure designed for and exposed to multiple hazards based on the current code requirements may not achieve the implied level of safety of the code for individual hazards (Crosti et al. 2011). This implies that safety for a multi-hazard event can be designed at lower level than what is intended by the code. Part of the reason such an event could occur is due to the current envelope method used in design.

In the envelope method of design, a structure is designed for actions that are the most severe for different load combinations. Based on this design method, it is estimated that the risks of exceedance of limit states can be up to twice as much for regions with significant wind and seismic hazards as compared with regions where only one hazard dominates (Duthinh & Simiu 2009).

1.2.3 Interactions Between Traffic and Bridges

1.2.3.1 Traffic Load During Seismic

While many analyses and codes neglect to analyze a bridge's seismic response under a combination of vehicle live and earthquake loads, the concern is growing in recent years. One event that greatly inspired the interest of engineers was the derailment of the Joetsu Shinkansen bullet train on October 23, 2004, just south of Nagaoka City. The earthquake was a magnitude of 6.6 and was considered to be the most devastating earthquake in Japan since the 1995 Kobe Earthquake (Kim et al. 2011). Many of the studies rooted from this event looked at the train/bridge interaction, but many of the principles and findings are common to vehicular live loading.

While most existing studies do not consider the vehicle live load in seismic design of bridges, one must consider the fact that considerable traffic usually remains on the bridge, including the possibility of a traffic jam, during a seismic event. This is especially true given the current limitation on earthquake forecasting technology. Traditional superposition concept is to predict the bridge response under both earthquake and traffic separately before being cumulatively added up. As a result, dynamic interactions of the bridge and traffic subjected to seismic cannot be considered. Existing studies on long-span bridges suggested a considerable impact from dynamic interactions of traffic, bridge, and other dynamic loads (Chen and Cai 2007). However, little information is available for short-span and medium-span bridges. While some codes do not account for this interaction of loads, one statistical study by Hida (2007) argues the excessive nature of the combinations in the AASHTO LRFD Bridge Design Specifications (2009). The argument is the load combinations in the AASHTO LRFD Specifications have not been calibrated on a statistical basis. Such a lack of statistical basis is then argued to lead to load factors that are unacceptably conservative (Hida 2007). Although, generally speaking, large conservatism usually leads to more robust structures with additional costs, conservatism for one member cannot guarantee the same conservatism at another member.

Over the years, traffic has become increasingly dense and vehicles have tended to become larger and heavier. The trend of increasing vehicle masses coupled with new materials and improved design methods has led to more flexible bridges, as well as stronger interactions with vehicles (Green & Cebon 1994). Vehicle live loads are increasing in both mass and speed. Using a dynamic analysis that takes into account the speed of the vehicles and the dynamic interactions can result in considerably larger, but realistic, forces acting on the bridge (Kozar 2009).

Liu et al. (2011) analyzed the vibratory behavior of a suspension bridge due to moving vehicle loads with vertical support motions induced by earthquakes. The study modeled the vehicles as a row of equidistant moving forces while the earthquake movement is modeled as the vertical oscillation of boundary supports (Liu et al. 2011). The calculation procedure presented was in the form of two coupled nonlinear cable and beam equations. The knowledge gained from the study includes discovery of the interaction between moving loads and earthquakes motions, which significantly amplify the response of the bridge near the end supports (Liu et al. 2011).

Other studies have taken the bridge vehicle interaction a step further to also include the effects of wind for slender long-span bridges. In several studies by Chen et al. (2007 & 2010), a

methodology for incorporating the effects of the vehicle and bridge interaction along with wind effects was developed and validated. The work began with a study in which each vehicle was modeled as several rigid bodies in combination with axle mass blocks, springs, and dampers with the inclusion of wind and road roughness excitations (Cai & Chen 2004). The full interaction modeling, however, was too complex and computationally costly to analyze simultaneously. In light of this, the next study conducted by Chen & Cai (2007) proposed a two-part approach. The first part consisted of full single vehicle-bridge-wind analysis to predict the equivalent wheel loads on the bridge. In the second part, these equivalent wheel loads are used to analyze the bridge response using a bridge/traffic/wind system (Chen & Cai 2007). In order to consider more realistic stochastic traffic on the bridge, the stochastic traffic flow on the bridge is simulated with the cellular automata (CA) traffic flow model developed by Nagel and Schreckenberg (Chen & Wu 2010). The cellular automata traffic simulation model is based on a discretization of both time and space, and each lane is divided into cells that are equal in length. There are four main rules to define the movements and actions of traffic within the simulation (Nagel & Schreckenberg 1992). A combination of the equivalent dynamic wheel load (EDWL) approach and CA traffic model were utilized to incorporate stochastic traffic flows into the vehicle-bridge-wind interaction model.

With the advance of computers and computation tools, more researchers are using 3D FEM models to analyze the bridge's seismic response through time history analysis. Only a few studies have tried to solve the problem of seismic response of bridges incorporating the bridge-vehicle interactive effect, such as those studies by Kameda et al. (1992). Their study, however, only considered simple stationary vehicle loadings. Multiple lane loadings and the effect of moving vehicle loads were not pursued (Kim et al. 2011). More recent studies employed two methods to simulate the vehicle live load. One method is to add supplemental masses to the structure, as used in previous studies, and the other is to treat a vehicle as a dynamic system. The difficulties in employing a moving load analysis, however, are the multitude of input parameters to a solution. These inputs can include: axial force influence, moving mass, moving force, surface irregularities, etc. In a couple studies performed by Kim et al. (2011), it has been found that the seismic response of the bridge, when analyzing the vehicular live load as a dynamic system, reduces when compared with results from modeling the vehicle live load as additional masses (Kim et al. 2011). These studies go further by also showing the reduction in the seismic response of the bridge with the vehicular dynamic system in comparison to the design as specified in the code where the vehicle live load is neglected entirely (Kim et al. 2011). All these findings demonstrate the need for continued research in the analysis of bridge seismic response with the vehicle live load in coincidence.

1.2.4 Interactions Between Scour and Bridges

While bridge scour is one of the most common causes of bridge failure, the research effort of combining scour and flood events with seismic analysis is still new. Only a few studies have been conducted and published, a noteworthy one of which was conducted by Alipour et al. (2011). While the need for the design of bridges against the effects of scour and structural degradation is intuitive, AASHTO code does not require such consideration directly. In the AASHTO LRFD code, scour is not a load to be considered, but rather is incorporated in the environmental conditions in order to ensure the structure is not vulnerable to extreme loads (Alipour et al. 2011).

Scour is defined as the water-induced erosion of soil around the foundation of a bridge. It contains three different forms: long-term aggradation and degradation of the river bed, general scour that can be caused by a contraction of the flow, and local scour due to an acceleration of water at the abutments and piers (Alipour et al. 2011). It is worth mentioning that the local scour has been evaluated to be the most significant of the three forms and should warrant the most attention in research. Another logistic of this research problem is in calculating the scour depth. While there are several equations to calculate the scour depth, the most common one is the Federal Highway Administration's (FHWA) equation in the Hydraulic Engineering Circular No. 18. This equation uses flow depth directly upstream and also incorporates correction factors for several different parameters of the stream flow in relation to the bridge pier (Alipour et al. 2011). With consideration given to the scour type and depth, the analysis can move on to developing fragility curves for the scour and seismic event.

Alipour et al. (2011) performed case studies on a two-span bridge and a three-span bridge. The soils were modeled with bi-linear (p-y) springs along the length of the pile shafts using the values for axial load and deflection from the American Petroleum Institute (Alipour et al. 2011). The fragility curves for these case studies were developed based on Monte Carlo simulations of 10,000 cases. These simulations were more specifically used in order to find the probability of occurrence of different scour depths during a 100-year return period event (Alipour et al. 2011). Once these depths and their respective probabilities were estimated, the soil springs in the depth of scour were removed for seismic analyses.

The bridges were subjected to a suite of 60 ground motions developed from the FEMA/SAC project (Alipour et al. 2011). With the incorporation of a Performance Based Design (PBD) framework, utilizing the fragility curves and ductility measures, it was possible to develop a complete picture about the risk of the bridges subjected to multiple hazards. It was noticed that as the scour occurs, the length of the bridge pier increases. With the increased effective length, the bridge is more flexible. This increase in flexibility leads to larger deformations in a given seismic event (Alipour et al. 2011). As can be seen in this study by Alipour et al. (2011), the occurrence of a seismic event after scour events leads to an increase in probability of failure. More studies are still needed to provide better insight of the joint effect of seismic and scour.

1.3 MOTIVATION OF THE PRESENT STUDY

The purposes of this study are to (1) develop a general analytical methodology to study multiple service and extreme loads for short- and medium-span bridges, and (2) conduct numerical performance analysis of a typical bridge in a mountainous region subjected to seismic and other extreme and service loads, including scour and stochastic traffic. This is achieved through the formulation of a detailed FEM-based modeling of a typical concrete multi-span bridge in Colorado, and realistic modeling and quantification of traffic service loads and the rational consideration of the associated dynamic interactions with the bridge. To evaluate the performance of the bridge under combined dynamic loads, time-domain nonlinear analysis is carried out. The objectives were broken down into the following tasks, described below.

First, the detailed FEM model of a typical medium-span pre-stressed concrete bridge in Colorado is developed with SAP 2000. Second, the stochastic traffic flow on the bridge is simulated with

the advanced traffic flow simulation tools. The dynamic time histories of moving wheel axle loads are quantified considering dynamic interactions. Third, the time histories of moving vehicles with interactions effects are applied on the corresponding nodes of the FEM model to simulate the dynamic traffic stochastic loads. Fourth, a collection of different scenarios of combined extreme and service loads, such as seismic, traffic, and scour, are studied to assess the bridge performance. In order to include the dynamic loads from the moving traffic, the FEM models of the bridges will include detailed superstructures to provide more detailed performance information. In addition, the following study will also attempt to shed light on and quantify the effects of pier elongation from scour events in combination with the seismic performance of the typical highway bridges being modeled.

1.4 ORGANIZATION OF REPORT

The report is composed of five sections. In Section 1, pertinent background information and literature review results related to the present study are introduced. In Section 2, the detailed information of the bridge being modeled as well, as the FEM modeling results with SAP2000, is presented. In Section 3, the stochastic traffic load acting on the bridge and the scour prediction are studied. In Section 4, the bridge performance under various load scenarios with different combinations of different extreme and service loads is investigated and some findings are discussed. The report concludes with Section 5. This section offers a summary of the findings and some conclusions that can be drawn from the previous sections.

2. BRIDGE MODELING WITH SAP2000

2.1 INTRODUCTION

The following chapter is a description of the modeling process of a typical concrete bridge located in Colorado. The commercial software SAP2000 version 15.0.1, produced by Computers & Structures Inc., was used to conduct the bridge modeling and seismic analysis.

2.2 DESCRIPTION OF BRIDGE

The bridge selected and modeled for this study was a simple overpass, symmetric, two-span prestressed concrete box-girder bridge. This particular bridge is located in the northern part of Thornton, Colorado, just north of Denver. The superstructure of the bridge consists of 23 concrete box-girders, which supports an 8" reinforced concrete deck. Construction drawings show this bridge was constructed as two simple support spans that were converted to a continuous connection type through a monolithic connection with the deck. The two spans are equal at a length of approximately 127 ft., giving a total bridge length of 254 ft. The overpass carries five lanes of traffic in each direction with each lane 12 ft. wide. In total, the bridge is 147 ft. wide from an outside edge of the rails to the other. Both abutments situated at the east and west ends of the bridge are integral abutments and are supported on caissons and retaining walls. At the bent, the superstructure is supported by eight 72 in. by 48 in. elliptical piers. Each pier is supported by 54-inch diameter circular concrete caissons. Figure 2.1 shows a plan layout of the 104th Street Bridge and Figure 2.2 is an elevation view of the bridge.

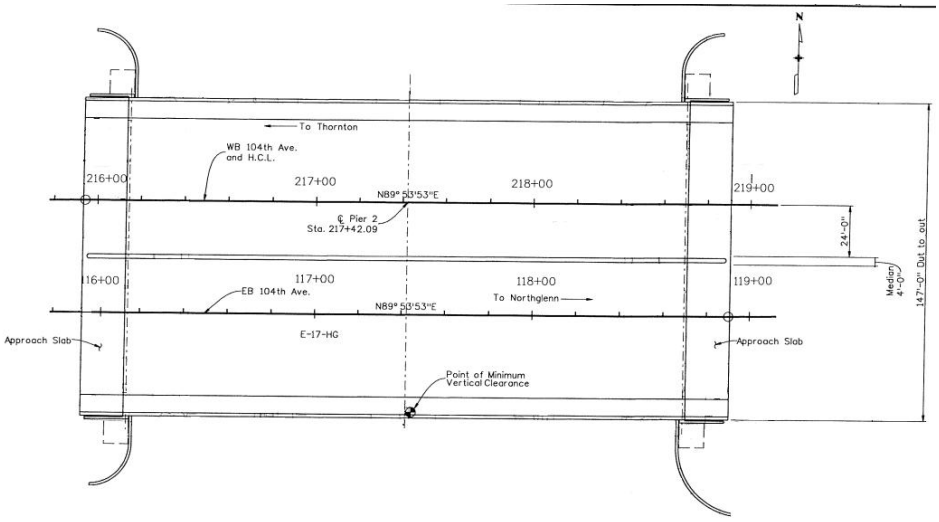

Figure 2.1 The Plan View of the 104th Bridge

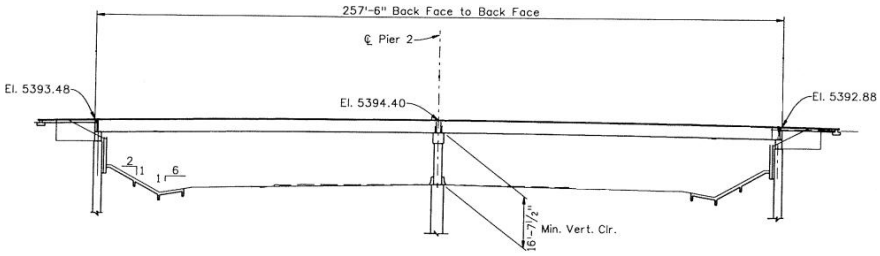

Figure 2.2 The Elevation of the 104th Bridge

A finite element model of the 104 Bridge was created in SAP2000 (Fig. 2.3) (CSI 2011). The bridge deck was modeled using a network of shell elements, representative of the concrete section and embedded top and bottom steel reinforcement. The box girders were modeled using frame elements, with prestressed tendons modeled as freestanding loads. The substructure, including the bent cap, columns, and caissons, were modeled with frame elements and connected via rigid links at appropriate locations. A further review of the modeling process is provided below.

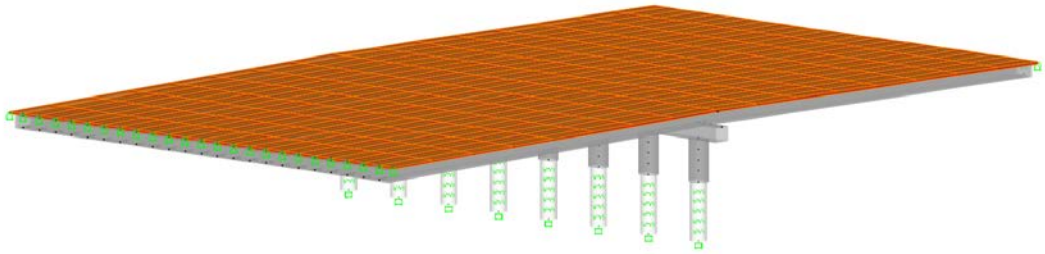

Figure 2.3 Rendered View of the 104th Bridge Finite Element Model

2.3 MATERIAL MODELING

The modeling process used in this study follows the procedures utilized by the Washington State Department of Transportation (WSDOT), shown in their Bridge Design Manual for seismic analysis (WSDOT 2012).

The 104th Bridge model consists of five different material definitions. These materials consist of four different concrete definitions and one steel rebar definition. The breakdown for concrete materials is due to different unit weights being utilized based on the section the material is used for. Table 2.1 gives a breakdown of the materials and their unit weights.

Table 2.1 Material Definitions of the 104th Bridge

			Material Unit Weight [pcf]	
Material Name	**Material Type**	**Section Property**	**Dead Load**	**Modulus of Elasticity**
4500Psi – Deck	Concrete	Deck	155	150
4500Psi – Other	Concrete	Bent Cap	150	145
4500Psi – column	Concrete	Bent Columns	150	145
8500Psi – Girder	Concrete	Girders	165	155
ASTMA709 – Grade 50	Rebar	Rebar	490	—

The unit weights for dead load purposes are those used for the weight per volume in the material definition form. Moduli of Elasticity unit weights are those values used in determining the Modulus of Elasticity as in the ACI Code Section 8.5.1, shown as Equation 2.1 (ACI Committee 318 2008).

$$E_c = w_c^{1.5} * 33 * \sqrt{f`_c(psi)} \qquad \text{Equation 2.1}$$

In Equation 2.1, the w_c value is the unit weight of the material in pcf and $f`_c$ is the compressive strength of the concrete in units of psi. All concrete materials used a Poisson's Ratio of 0.2 and a Coefficient of Thermal Expansion of $6.00*10^{-6}$ in./in./ºF. The steel material utilized a Modulus of Elasticity of 29,000 ksi, a Poisson's Ratio of 0.3, and a Coefficient of Thermal Expansion of $6.50*10^{-6}$ in./in./ºF. The bent columns, expected to behave inelastically, must be defined for the nonlinear range. Bent columns are defined to use a Mander confinement model and unconfined compressive strains of 0.002 in./in. and 0.005 in./in. at the unconfined compressive strength and ultimate capacity, respectively. The two strain values are in accordance with Section 8.4.4 of the AASHTO Guide Specifications for LRFD Seismic Bridge Design (American Association of State Highway and Transportation Officials 2009).

2.4 SUBSTRUCTURE MODELING

The following two sections give detailed descriptions of the modeling process for the bent columns and bent caps for the 104th Bridge.

2.4.1 Column Modeling

The 104th Bridge is a two-span bridge, containing only one bent, which contains eight elliptical bent columns, all of which are at the same height. These bent columns are 72 in. by 48 in. in overall dimension. The compressive strength of the concrete material is 4500 psi, and incorporates the Mander confinement model for the core concrete in the section. The column section is geometrically modeled in SAP 2000 through a predefined Caltrans shape. One core is used in the section with a cover of 2-5/8 in., including (20) #9 bars and a hoop confinement definition of a #5 bar at 12 in. on-center. In the unconfined region surrounding the inner core are (12) #9 bars arranged in an elliptical manner. Figure 2.4 illustrates the cross section of the bent column.

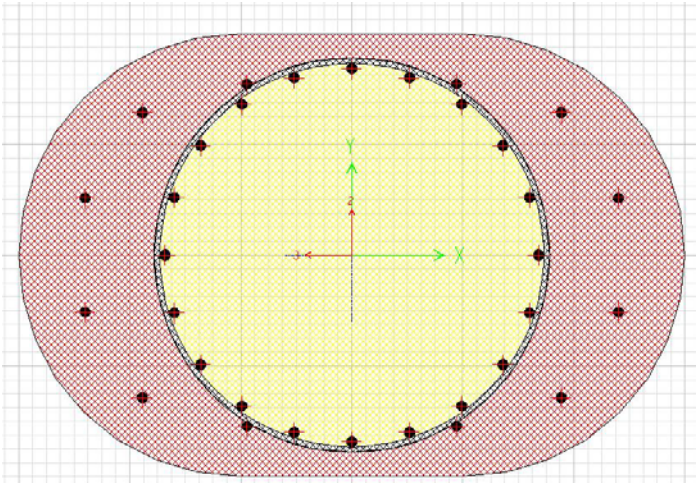

Figure 2.4 Column Section of the 104th Bridge

While Figure 2.4 depicts the general bent column section, other sections are also utilized in order to model the transitions and splicing of rebar between the bent column and the caisson. The bottom five feet of the bent column has double #9 bars in a perimeter manner in the inner core. The eight elliptical columns are broken into six segments, which satisfy the requirement of Section 5.4.3 of the AASHTO Guide Specifications for LRFD Seismic Design of a minimum of three elements (American Association of State Highway and Transportation Officials 2009).

2.4.2 Bent Modeling

The bent cap is modeled using a frame section with uniform x-section that is 48 in. high and 58 in. wide. The compressive strength of the concrete is 4500 psi and includes a reinforcement cover of 3 in. The section contains (12) #11 bars in two layers of six bars each at the top and bottom of the section. On each side of the section are (5) #5 bars evenly spaced between the layers of #11 bars at the top and bottom of the section. In total, there are (10) #5 bars in the section. The inner core is confined with #5 hoops at 6 in. on-center.

Figure 2.5 depicts the 104th Bridge bent section. Another aspect of the bent modeling is the connection between the bent column and the bent cap. This particular model utilizes the rigid link connections in SAP2000. The procedure for this connection is to tie adjacent nodes together at the interface of the bottom of the bent and the top of the column via a rigid link that restrains translation and rotation in all degrees of freedom.

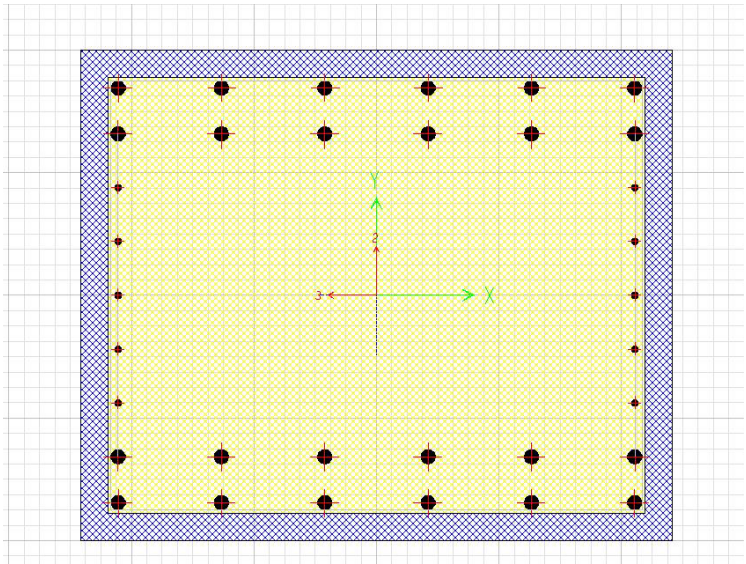

Figure 2.5 Bent Section of the 104th Bridge

2.4.3 Foundation Modeling

Soil-structure-interaction (SSI) effect is not considered in this study given the typical soil conditions in mountainous areas. The procedure utilized in defining the foundations in the model is more simplistic and focuses on the physical nature of the connections at the soil and structure interface.

While the 104th Bridge is an integral abutment bridge (IAB), it was decided to model the bridge as a bearing type in order to give more general insights. It is known that bearing support is more common on bridges in moderate seismic zones, and such a decision was made in hopes of finding more typical results for construction within the region of study. At each abutment the translation in the transverse and vertical directions are fixed while longitudinal displacements are allowed. All rotational degrees of freedom are released at the abutments. The bent-columns are supported by caissons that are embedded into the soil down to the bedrock. The resistance provided by the soil on the caisson was modeled using linear springs, developed using existing methods found in research and code design examples (FHWA 2004). The embedment of the caissons into the bedrock was represented with complete nodal fixity, restraining translation and rotation in all degrees of freedom.

2.5 SUPERSTRUCTURE MODELING

One of the important components of the structural model is the representation of the superstructure. Many bridge studies utilize a simple superstructure model due to the majority of the mass being in the substructure and the assumption of elastic behavior in the superstructure. In this study, a more detailed approach is taken to model the superstructure in order to assess the effects of multi-hazard events on the superstructure as well as to incorporate the traffic live loads in conjunction with the seismic time histories.

2.5.1 Girders

2.5.1.1 The 104th Bridge over Interstate I-25

The 104th Bridge is composed of 23 prestressed box girders. Each box girder has overall dimensions of 46 in. deep and 72 in. wide. It follows that the overall width of the girders and deck are 138 ft. wide. The complexity of the overhangs was neglected, as the added dead load is minimal. Modeling the width of all girders and the 8 in. deck on top of the girders allows for the live load and investigation into the superstructure. The girders have 4 in. of flange thickness and 6 in. of web thickness, and are composed of 8500 psi concrete. Figure 2.6 illustrates the girder cross section.

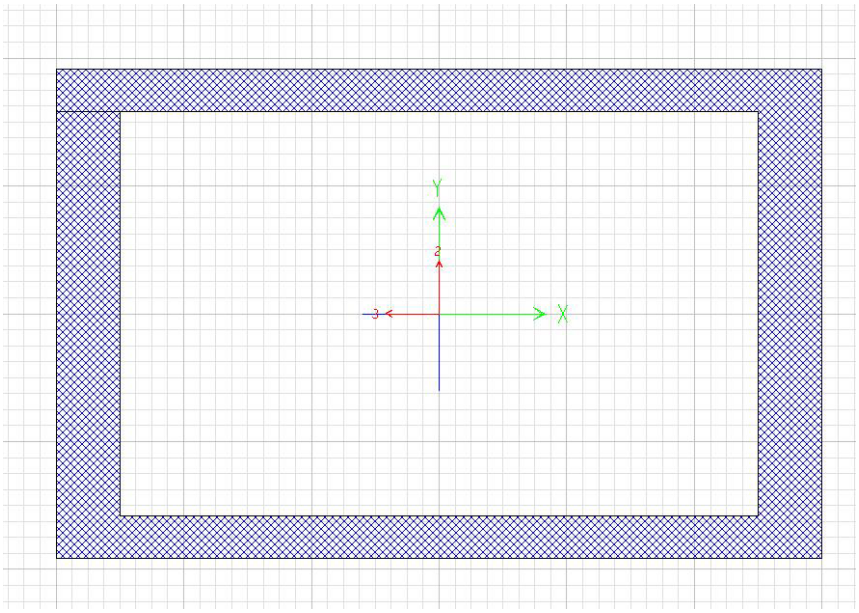

Figure 2.6 Girder Section of the 104th Bridge

Another aspect of the superstructure modeling is in the connections at the bent. According to the construction drawings for the 104th Bridge, the bridge is a simple support converted to continuous through the use of a monolithic deck. In order to effectively model the connection in its service state, a rigid link connection between the superstructure and bent is utilized.

2.5.2 Deck

The modeling of the deck is undertaken in the present study to gain a certain amount of resolution in the superstructure. The deck is composed of 4500 psi concrete, with embedded top and bottom reinforcement. Due to the minimal contribution to the performance of the bridge structure, the reinforcement was neglected in the analysis. The deck, like the girders, is segmented into eight sections in the length of each span. An area section is defined in SAP2000, utilizing a thin shell section type of 8 in. depth. Each deck element has the length, in the longitudinal direction, equal to the girder segment length and a width, in the transverse direction, equal to the spacing of the girders. The nodes corresponding to the centroid of the deck are the same as the nodes used for the insertion of the girders.

2.6 HINGE MODELING

The hinge modeling process contains several steps. The plastic hinges are used both in the non-linear time history load cases and the pushover load cases. Defining and assigning the hinges require three main steps of calculating column inflection points, calculating plastic hinge lengths, and assigning the plastic hinges (WSDOT 2012).

In order to first calculate the column inflection points, it is required that the dead load case be run. This step is necessary since the plastic moment capacities of the columns under dead load will be utilized to calculate the location of the inflection points (WSDOT 2012). Once the dead load is analyzed, the axial force in the columns, both at the top and base of the column, are measured. An idealized Caltrans curve is also used to calculate the plastic moment for a section with the input of an axial load. Table 2.2 shows the axial loads and the plastic moments for the columns of the 104th Bridge. The columns are numbered from the North and only the first four columns are shown due to the symmetry of the bridge.

Table 2.2 Column Properties of the 104th Bridge

Column	Location	Axial Load [kip]	Plastic Moment [kip-in.]
1 & 8	Top	-576.2	39,578
	Base	-619.0	55,335
2 & 7	Top	-990.2	45,137
	Base	-1033.0	60,229
3 & 6	Top	-961.0	44,706
	Base	-1003.7	60,207
4 & 5	Top	-942.7	44,650
	Base	-985.4	59,978

With the plastic moments and a clear height (L_c) of 202.5 in. for all bent columns, Equations 2.2 and 2.3 are used to calculate the distance from the point of maximum moment at the base of the column to inflection point in inches and distance from the top of column to point of inflection in inches, respectively. Both equations are from the *WSDOT Bridge Design Manual* (WSDOT 2012).

$$L_1 = \frac{L_c * M_{p\_col\_base}}{\left(M_{p\_col\_base} + M_{p\_col\_top}\right)} \qquad \text{Equation 2.2}$$

$$L_2 = L_c - L_1 \qquad \text{Equation 2.3}$$

The next step in the process of hinge modeling is to calculate the hinge lengths. Plastic hinge lengths are calculated at both the base and top of the bent columns. The plastic hinge length equation used for the present study is taken from Section 4.11.6 of the *AASHTO Guide Specifications for LRFD Seismic Bridge Design* and is presented as Equation 2.4 (American Association of State Highway and Transportation Officials 2009).

$$L_p = 0.08 * L + 0.15 * f_{ye} * d_{bl} \geq 0.3 * f_{ye} * d_{bl}$$ Equation 2.4

In Equation 2.4, L is either L_1 or L_2 from Equation 2.2 or Equation 2.4, depending on which plastic hinge is being considered. The variables f_{ye} and d_{bl} are the expected yield strength of the longitudinal reinforcement in kips per square inch and the diameter of the longitudinal reinforcement in inches, respectively. A minimum plastic hinge length must be examined in accordance with the code and is seen as the second part of Equation 2.4 above. This minimum value of 16.9 in. for the 104th Bridge model was found to govern in all cases.

The final step in the hinge modeling process is to assign the plastic hinges to the columns at the right locations. In order to assign hinges to a frame element, the relative length within the element is needed for locating the hinge. Once the relative length for the hinge location is estimated and the frame element is selected, SAP2000 allows the user to define the hinge properties. The present study utilizes the capacity of SAP2000 to create automatic hinge properties based on Caltrans Flexural Hinge properties. Two hinges are utilized at both the base and top of the column, resulting in four hinges per column. The need for two hinges is due to the definition of the hinges as a P-M2, axial and moment in the local 2 direction of the element, or P-M3, axial and moment in the local 3 direction of the element, hinges. This procedure, along with selecting that the deformation drops after reaching Point E on the curve, is based off the *WSDOT Bridge Design Manual* seismic example (Washington State Department of Transportation 2012).

2.7 MODAL ANALYSIS

The mass source is defined from the dead load of the structure. The modal analysis load case is also modified from the SAP2000 preset definitions. The analysis starts from an unstressed and zero initial conditions state. Modes are based on Ritz Vectors, not the conventional Eigen Vectors, for increased accuracy. The Ritz Vector method increases the accuracy since it takes into account the spatial distribution of the dynamic loading (Computers & Structures, Inc. 2010). The maximum number of modes found is 30 to ensure the modal participating mass ratios are greater than 90% in both directions to meet requirements of Section 5.4.3 of the *AASHTO Guide Specifications for LRFD Seismic Bridge Design* (AASHTO 2009).

Modal analysis was conducted on the 104 Bridge using Ritz vectors for participation in the first 35 modes. Longitudinal vibration was induced in the first mode (shown in Figure 2.7) at a vibrational period of 0.894 seconds. Vertical and translational vibration is primarily induced for the second and third mode shapes, respectively.

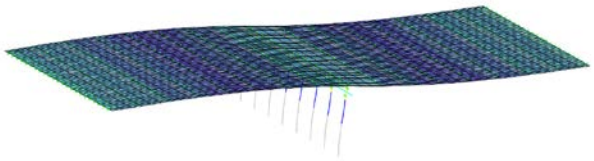

Mode 1 – Longitudinal Vibration T = 0.894s

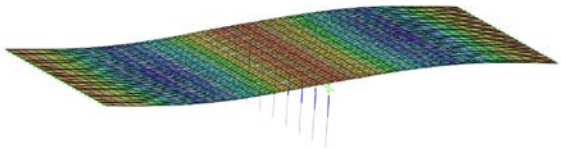

Mode 2 – Vertical Vibration T = 0.516s

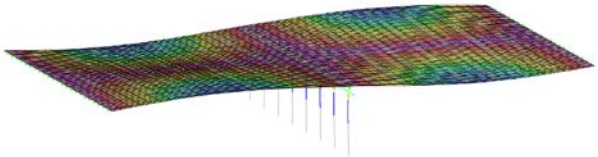

Mode 3 – Torsional Vibration T = 0.489s

Figure 2.7 Mode Shapes

2.8 NON-LINEAR DYNAMIC TIME HISTORY ANALYSIS

Dynamic time history analyses are considered as a type of more rigorous analysis case, and require several analysis steps. The time history analyses in this study use the Hilber-Hughes-Taylor method of direct integration in SAP2000. The nonlinear time history case is continued from the physical state of the bridge prior to an earthquake under dead load, rather than a zero initial condition state. In the present study a direct integration analysis was utilized, which allows for the time stepping method of solution.

3. BRIDGE SCOUR PREDICTION AND TRAFFIC LOAD SIMULATION

3.1 INTRODUCTION

This section introduces the efforts on defining the traffic loads and scour models for the present study.

3.2 TRAFFIC LOADING

The traffic flow for the 104th Bridge is determined by the Cellular Automaton (CA) traffic flow simulation based on some site-specific traffic information. The CA model, a microscopic scale traffic flow simulation model, is able to provide detailed instantaneous information of each vehicle through replicating major traffic phenomena on highways.

3.2.1 Rules of CA Traffic Flow Model

The CA traffic model is based on the assumption that both time and space are discrete and each lane is divided into cells with an equal length as shown in Figure 3.1. Each cell can be empty or occupied by, at most, one vehicle at a time. The velocity of a vehicle can be determined by the number of cells a vehicle can move during one time step. The maximum velocity a vehicle can achieve is defined based on the actual speed limit on the road. At each time step, a vehicle moves, accelerates, decelerates, or changes lanes based on some predefined rules. The rules are typically established according to the actual traffic rules with some reasonable assumptions of the driver behavior (Nagel & Schreckenberg 1992).

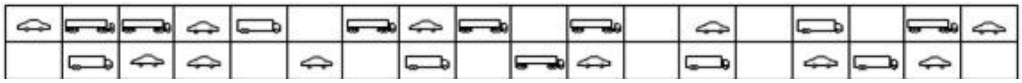

Figure 3.1 CA Discretization Model

The rules of a typical CA traffic model include: 1) rules for vehicles moving forward on the original lane, i.e. single-lane CA model; and 2) rules for changing lanes, i.e., multiple-lane CA model. The rules of the single-lane CA model, shown in Figure 3.2, include (Nagel & Schreckenberg 1992):

(1) Acceleration: if the velocity of Vehicle v is smaller than v_{max} (maximum velocity a vehicle is allowed to achieve) and if the distance to the next vehicle ahead is larger than $v+1$, the velocity is advanced by one;
(2) Deceleration: if the vehicle at site i finds the velocity of the next vehicle at site $i + j$ with j not larger than v, it reduces its velocity to $j-1$;
(3) Randomization: with the probability of pb, the velocity of each vehicle is decreased by one if the velocity is greater than zero;
(4) Vehicle motion: each vehicle advances v sites.

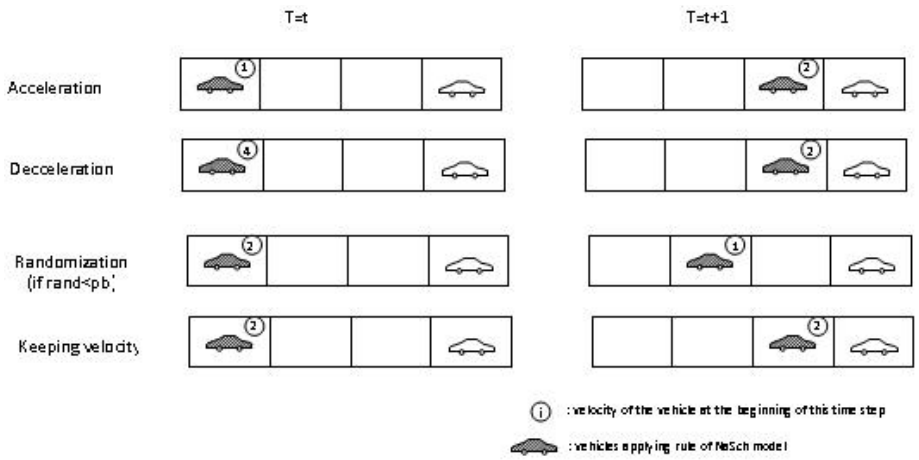

Figure 3.2 Single Lane CA Model Rules

The rules for multiple lane CA models and lane changing are shown as follows in Figure 3.3 (Rickert et al. 1996; Chen and Wu 2011).

(1) The distance (described as "*gap*") between one vehicle and the vehicle right ahead on the same lane is less than *v+1*, i.e. the vehicle cannot accelerate in the current lane;
(2) The distance (described as "gap_o") between one vehicle and the vehicle ahead on the target lane (i.e., the neighboring lane) is more than *v+1*, i.e., the vehicle can accelerate if it changes lane;
(3) The distance (described as "$gap_{o,\,back}$") between the vehicle and the behind vehicle on the target lane is more than v_{max}, i.e., the vehicle will not crash with the vehicle on the target lane;
(4) With the probability of *pch*, a vehicle changes lanes if all the three above conditions are satisfied.

To fulfill the lane-changing simulation, the location and the velocity of Vehicle *i* will be updated through two sub-steps: 1) Vehicle *i* moves to the target lane transversely without moving forward; and 2) Vehicle *i* moves forward obeying the single-lane rule as introduced above after moving into the target lane.

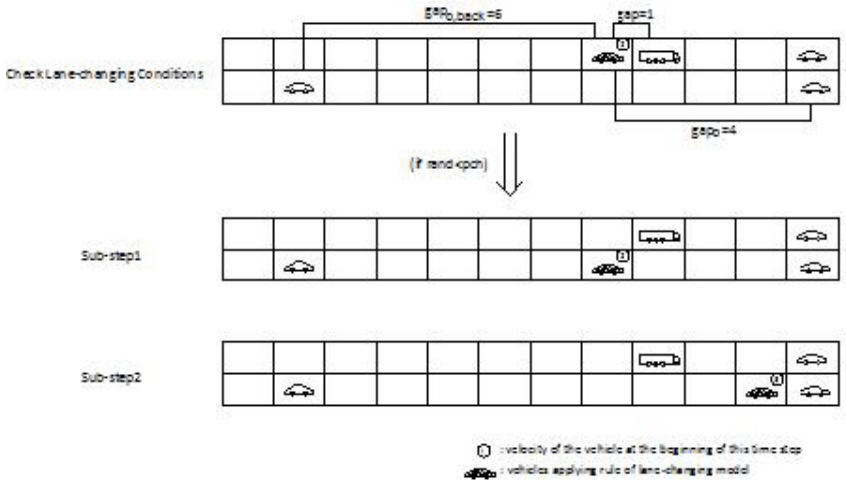

Figure 3.3 Lane-Changing Rules

3.2.2 CA Traffic Model Parameters for the 104th Bridge

The following list depicts all of the parameters used in the CA Traffic model of the 104th Bridge used in the present study.

Length of each cell: 7.8m
Number of cells on the bridge: 10
Traffic density (busy): 32 veh/km/ln
The probability of braking: 0.5
The probability of changing lane: 0.8
Three types of vehicles: sedan(v1), light truck(v2), heavy truck(v3)
Percentage of v1, v2 and v3, respectively: 20%, 30%, 50%
Weight of v1, v2 and v3, respectively (N): 15788, 47726, 245690

3.3.3 Generation of traffic Load Time Histories

The 104th Bridge has three through lanes and two turn lanes in both positive and reversed driving directions, thus the CA traffic model for the current bridge has five lanes in each direction. The loading points for the bridge model are selected as the quarter points of each span of each girder. In total, there are 189 traffic loading points on the 104th Bridge model. Dynamic interaction analysis is conducted to consider the bridge-vehicle interaction analysis following the equivalent wheel loading approach (EDWL) (Chen and Cai 2007) and also the combined load approach (Chen and Wu 2010). The details of the approach are not repeated here, and only the basic steps are briefly introduced in the following.

The traffic load time histories are generated in the following three steps:

1. Establish the CA traffic flow model for the current bridge based on the traffic rules for both single-lane model and multi-lane model.
2. Determine the traffic loads for each lane at each time step based on the instantaneous location of vehicles according to the CA traffic model.
3. Distribute the traffic loads at each time step proportionally in both the longitudinal and transverse directions to the selected loading points.

In this study, the CA traffic flow is simulated for 60 seconds. The traffic time history of each loading point has 6,000 steps with a time step of 0.01 second. The unaltered traffic load history at the fourth loading point of the sixth girder is illustrated in Figure 3.4.

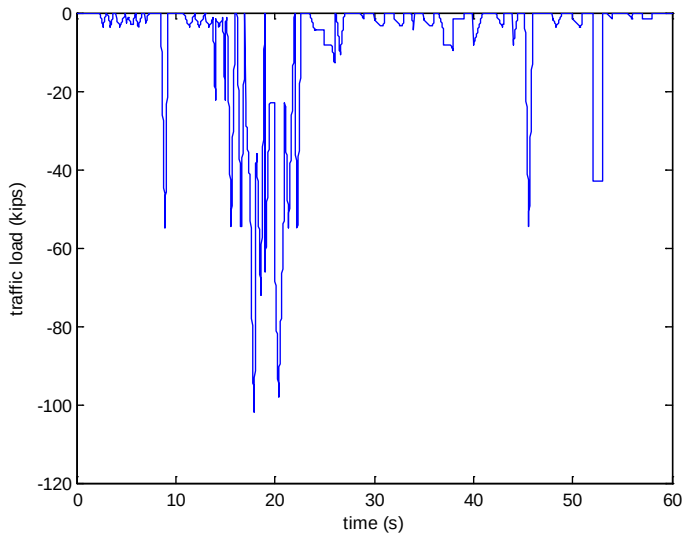

Figure 3.4 Traffic Load History of Fourth Node on Sixth Girder

3.3 SCOUR PREDICTIONS

The scour study in the present work was based on a parametric study, and the parameter of interest was the scour depth. Based on other studies investigating bridge scour, depths of 2.5m and 5m were chosen for the earthquake simulations. Corresponding models were made to reflect these scour events by removing the corresponding soil springs and subsequent resistance forces of the springs.

4. ANALYTICAL INVESTIGATION OF BRIDGES SUBJECTED TO MULTI-HAZARD SITUATIONS

4.1 INTRODUCTION

The following chapter presents and discusses the results of the 104th Bridge detailed model subjected to multiple extreme and service loads.

4.2 SELECTION OF GROUND MOTION

In order to simulate typical earthquake intensity in a moderate earthquake hazard region, a representative site location in Portland, Oregon, is selected with a stiff soil condition. A design response spectrum is developed using the United States Geological Survey (USGS) ground motion tools per the AASHTO Guide Specifications for LRFD Seismic Bridge Design (2009). Three representative earthquake records are chosen that are characteristic of an inter-plate tectonic setting and stiff soil condition (Table 4.1). The multi-hazard evaluation also considers vertical ground motion of which the contribution of each record is varied and increases with shorter site distances.

Table 4.1 Three Representative Earthquake Records

Record	Year	Mw	Mechanism	Significant Duration (s)	Site Distance	Vs30 (mph)
Northridge – Arcadia Campus Dr.	1994	6.69	Reverse	18.7	41.4	822.1
San Fernando – LA Hollywood Stor. FF	1971	6.61	Reverse	11.9	22.8	708.0
New Zealand – Matahina Dam	1987	6.60	Normal	6.3	16.1	950.3

4.3 EARTHQUAKE RESPONSE

Nonlinear time history analysis is conducted on the 104 Bridge using the Hilber-Hughes-Taylor method of direct integration. Rayleigh damping coefficients are employed in the analysis that represents 5% damping in the first and second modes. In the first analysis case, traffic loadings are subjected to the finite element model using a series of time-history load patterns. The traffic loading represents the mean intensity that the 104 Bridge would be subjected to on a day-by-day basis under standard, dry surface conditions. The traffic loading is applied subsequently to the dead load analysis, and for a time period duration of 40 seconds.

Displacement in the deck

Under the self-weight of the bridge, the observed displacement at the center of the first span is 0.75 in. and is consistent with the predicted camber specifications in the bridges superstructure design. With the application of dynamic traffic loading, the deck vibration increases the displacement to peak amplitude of 1.1 in. The distribution of traffic loading across the deck is neither uniform nor symmetric, shown by the induced vibration at the two exterior locations of span 1 (Figure 4.1a). The exterior edge shown, displays the largest observed deflection of 1.56

in. In the pier-columns of the substructure, the vibration of the deck induces drift, measured at the top of the column. The longitudinal drift (parallel to roadway) incurred in the pier-columns due to traffic loading is minor and does not exceed 0.05 % in either direction of bending (Figure 4.1b).

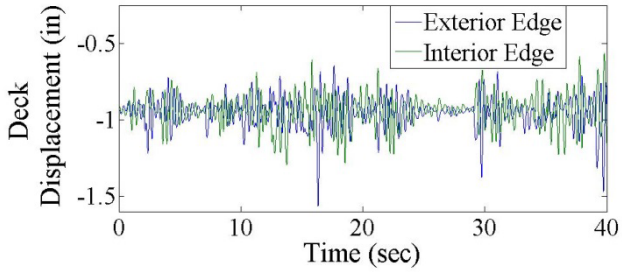

(a)

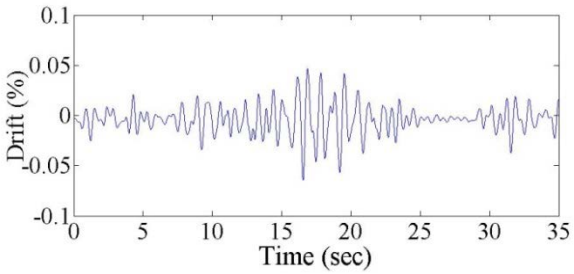

(b)

Figure 4.1 (a) Vertical Deck Displacement and (b) Longitudinal Drift of Pier-Columns

Substructure Demand

Under traffic loading, the distribution of demand on the substructure is uniform across the eight pier columns. The demand on column three (Figure 4.2) shows the distribution of forces throughout the piers and into the caisson. The distribution of moment in the longitudinal direction of the bridge is the largest at the top of the column and at the bottom of the caisson, as shown in Figure 4.2a. The maximum moment demands developed at the two respective locations are 277.8 kip-ft at the top of the column and 438.1 kip-ft at the bottom of the caisson. In comparison, at the axial load levels displayed, the capacities of the column and caisson to resist bending are 4,387.9 kip-ft and 3,076.5 kip-ft, respectively. The axial forces in the column vary with the intensity of the traffic loads, and the highest axial demand developed is 898.3 kips at the base of the columns. The shear forces, shown in Figure 4.2b, are minor and do not exceed more than 26 kips.

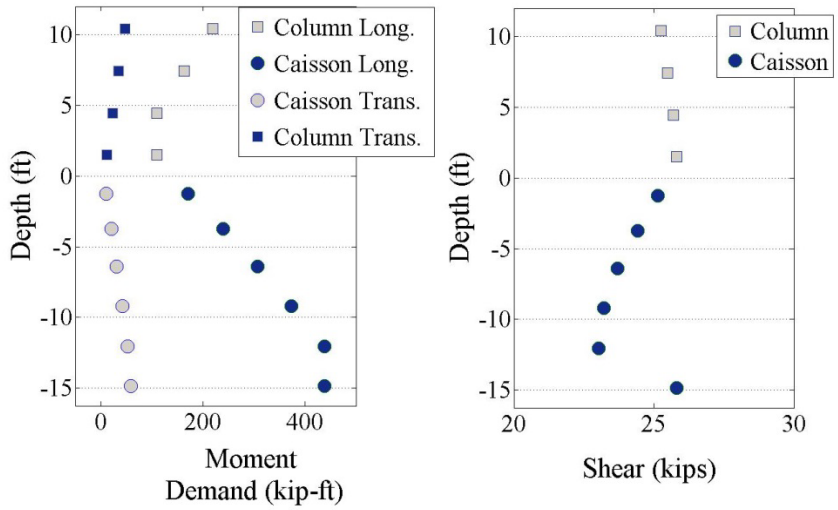

Figure 4.2 Distribution of (a) Moment and (b) Shear in the Substructure

Seismic and Traffic

In a moderate seismic region, a bridge may experience earthquake ground motion, which most frequently will stem from an inter-plate region. In the analysis, the 104 Bridge model is subjected to an earthquake record typical for an inter-plate tectonic setting together with the existing dead load and combined with dynamic traffic loading. Under the combined loadings, a notable increase in the deformed response and developed demand takes place. The earthquake employed in the analysis is the San Fernando Valley earthquake, recorded at the Hollywood Storage Building in Los Angeles. Only the results for one single earthquake are discussed; however, the same trends are observed in the results from other inter-plate earthquakes, including records from Northridge and Loma Prieta, for substantiation.

Ground motion excitation of the supports induces dynamic vibration of the deck with peak amplitudes of up to two inches observed in both the vertical and longitudinal directions (Figures 4.3a and b). This vibration corresponds to a subsequent 1.8% drift imposed on the pier-columns, which is significantly larger than what is observed under dead load and traffic conditions (Figure 4.3c).

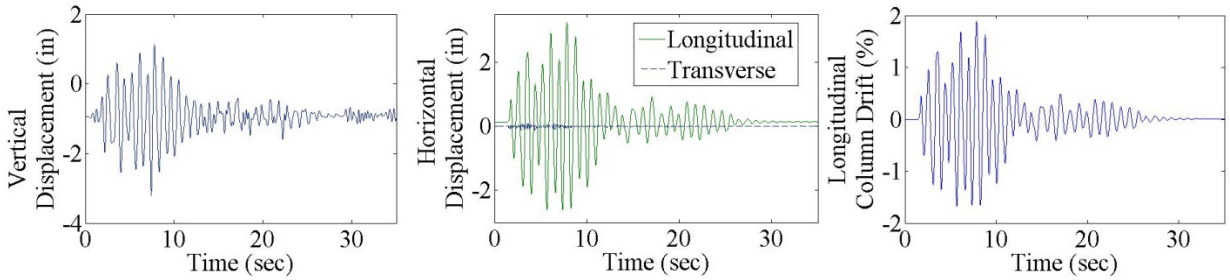

Figure 4.3 (a) Vertical and (b) Translation Displacement of the Deck; (c) Longitudinal Column Drift Ratio

The distribution of structural demand imposed by the earthquake is again uniform across the eight pier-columns. For each column, the largest bending forces are concentrated at the top of the piers; however the moment is more distributed to the bottom of the column in comparison with the traffic load case (Figure 4.4a). The highest concentration of moment in the caisson is at the bedrock, where exceedingly large moment demands are generated. At the top of the column, a moment of 4,632.25 kip-ft develops at the peak excitation of the earthquake. The moment at this location causes inelastic yielding in the column; however it does not reach exceedance of the ultimate capacity (Figure 4.4b). A strength degradation model is not used in the numerical analysis, which means the elastic stiffness is recovered after the section has yielded. For the means of this study, where large inelastic deformations are not reached, it provides a good approximate representation of the global substructure behavior. At the column bases where the demand is lower, the member remains elastic and does not undergo any inelastic deformation. Using the criteria developed in FEMA 2000, the inelastic deformation at the columns falls within the Immediate Occupancy limit state.

Large bending forces are developed in the caisson, particularly at the base, due to the extended lever arm to the superstructure where the seismic mass is concentrated. The base of caisson is embedded in bedrock and is therefore represented with a nodal constraint that imposes fixity in all six degrees of freedom. The result is a demand that would likely induce failure in the caisson and further research is suggested to quantify the possible failure. The forces generated may be unrealistic to an actual bridge where displacement and rotation of the caisson would realistically take place and alleviate a large portion of the demand generated.

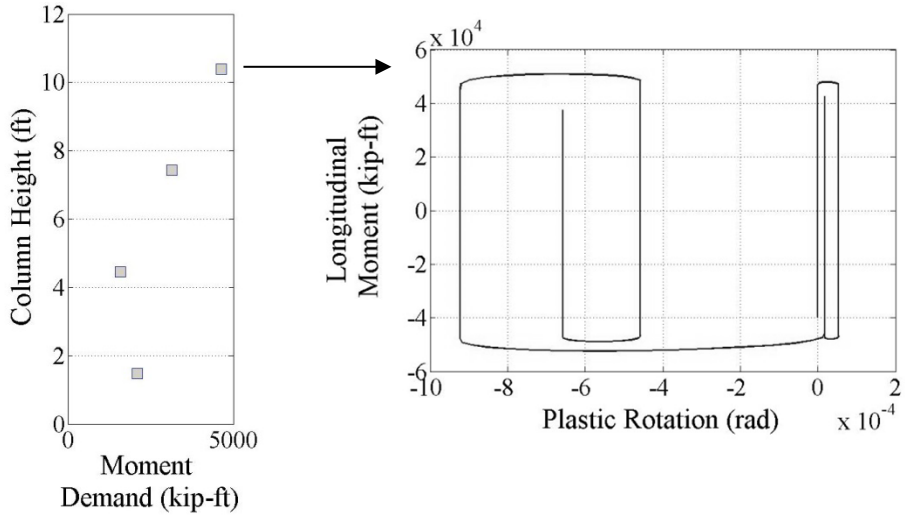

Figure 4.4 (a) Moment Distribution in the Column (b) Plastic Hinge Behavior

The longitudinal shear demand developed in the substructure reaches peak amplitude of 512.5 kips (Figure 4.5). The column capacity without any dynamic excitation is substantially larger. However, under ground motion excitation, the shear capacity-to-demand (C/D) ratio of the pier-column converges as the shear demand increases, and the capacity decreases due to higher bending forces and axial loads. The critical C/D ratio developed under ground motion excitation is 1.41.

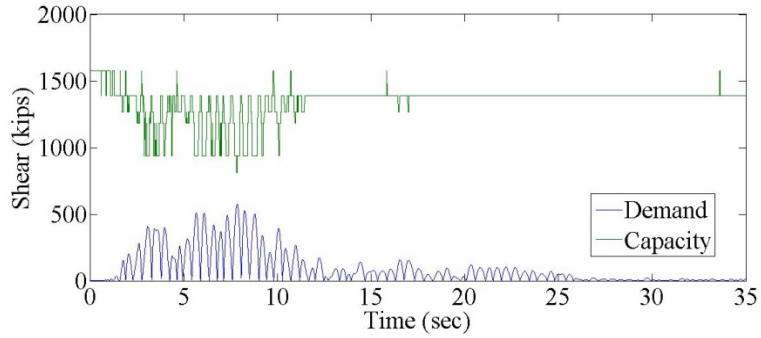

Figure 4.5 Shear Forces and Capacity of the Pier-Column

At the abutments, resistance is provided by the abutment supports in the vertical and transverse directions (Figure 4.6). The vertical dead load is resisted predominantly by the substructure, whereas the abutments yield a marginal contribution to providing support. The horizontal transverse seismic load is also resisted predominantly in the substructure; however, as seen in Figure 4.6, some resistance is provided across the abutment.

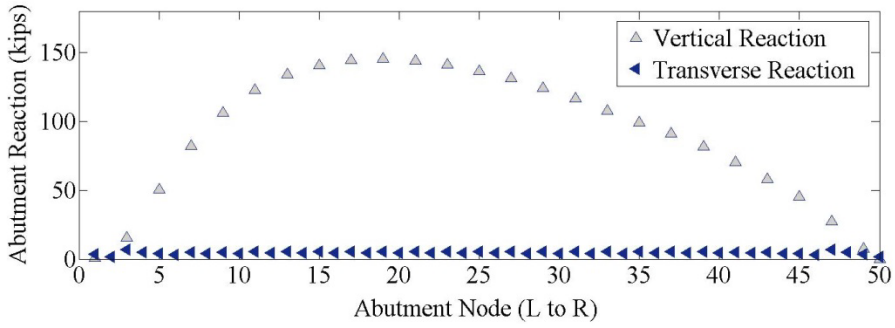

Figure 4.6 Abutment Supports Reactions

Effects of Scour

The effects of scour at the bases of the pier-columns were investigated by lowering the height of the embedded soil around the caisson. The investigation considers two cases, the first of which reduces the height of soil by 2.5 ft., while case two considers a larger reduction of 5 ft. The effect on the response of the bridge to combined seismic and traffic loading is considered.

The effect of scour on the column longitudinal drift, and vertical vibration of the deck, is negligible. The drift ratio, as shown in Figure 4.7a, does not exhibit a substantial resistance from the soil springs, compared with the stiffness of the column sections, thus the observed effect is minor. The moment imposed on the substructure is slightly reduced at the base and top of the pier columns as shown in Figure 4.7b. The reaction forces at abutments exhibit very small influences from scour. In comparison with the overall response to seismic loads, the inclusion of scour is substantially less influential. The hinge formed in the pier column of the bridge that does not include effects of scour, displays larger plastic rotations under cyclic loading (Fig. 4.8). In the load cases with increasing scour, the maximum hinge rotation developed under cyclic loading

decreases. The permanent deformation at the end of the load cycles, however, is larger. The increased permanent deformation in the hinge and overall decrease in moment demand is likely attributed to a decrease in the resistance force applied by the soil against bending.

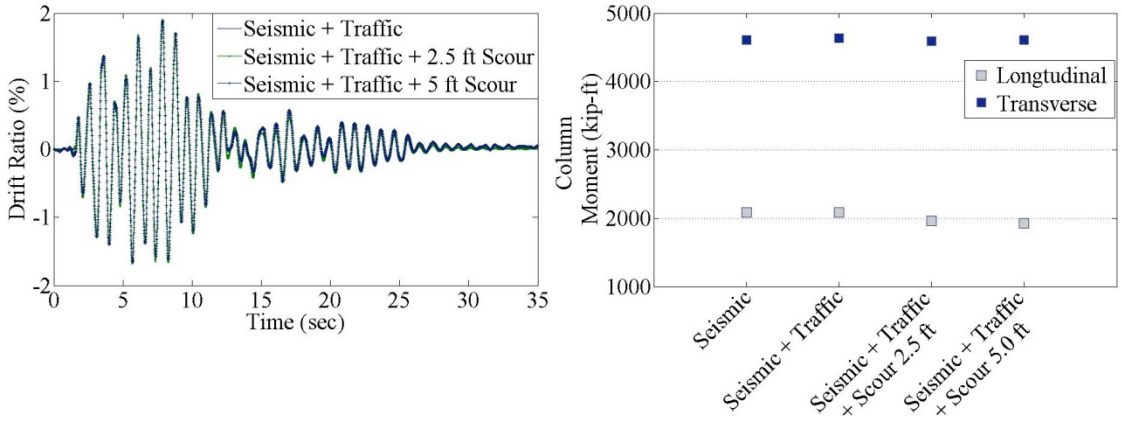

Figure 4.7 (a) Drift Ratios and (b) Moment Imposed on Column for Varying Scour Depths – Northridge Record

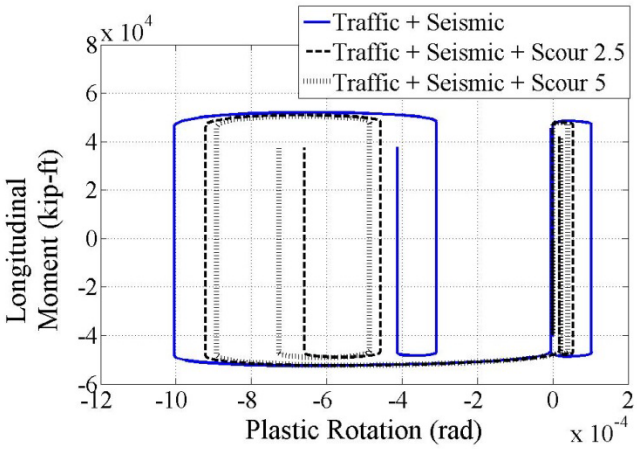

Figure 4.8 Plastic Hinge Behavior in the Column – Northridge Record

Effect of Vertical Ground Motion

For an active tectonic region, the vertical component of ground motion can be influential in certain cases. For this study, the more acute longitudinal component of the earthquake ground motion was applied in combination with the vertical component. The vertical ground motion component is scaled such that the original vertical-to-horizontal spectral acceleration ratio is maintained at the fundamental period of vibration.

Vertical ground motion excitation generally does not cause substantial effect on the bridge due to the inherent nature of the vertical component. With the applied loading in the vertical and longitudinal directions, the reaction and shear forces decrease in the transverse direction. Modal analysis of the 104 Bridge yields a fundamental period of vibration of 0.894 seconds, inducing a

predominantly longitudinal displaced shape. The inherent nature of the vertical earthquake component is concentrated at a short, high frequency band that is of a much higher frequency than the vibrational period of the bridge. The bridge is therefore relatively unaffected by the high frequency vertical excitation. As shown in Figure 4.9, the dynamic vibrations induced are relatively consistent with the dynamic vibrations induced by excitation in the translational directions.

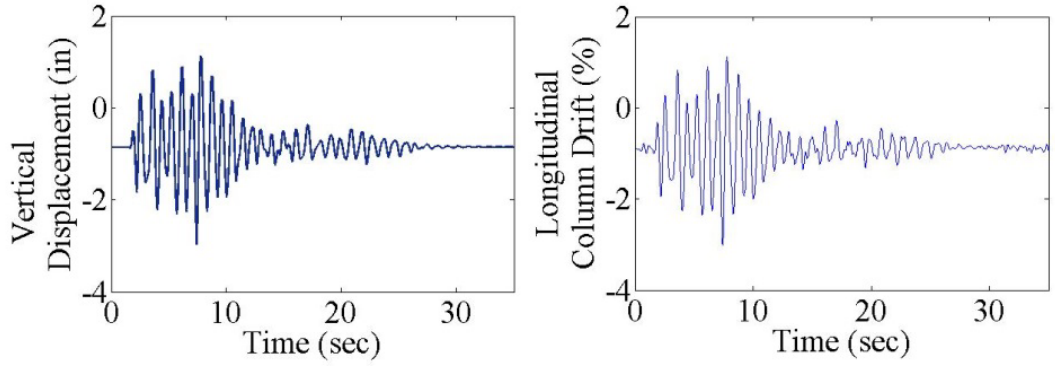

Figure 4.9 Vertical Displacement and Longitudinal Column Drift

Investigation of Spread Footing

The bending forces developed at the base of the caisson yielded demands that exceeded the capacity of the caisson section. In order to study the effects of employing a seismic resistant support, a spread footing was employed in the model. In the analyses, the spread footing is assumed to be sufficiently designed to resist both rotational and translational displacements at the base of the column. The finite element model is subjected to dynamic traffic loading in combination with the San Fernando earthquake.

The result of employing a spread footing causes a large reduction in the drift observed in pier-columns by restraining translation and rotation at the bases (Figure 4.10). Under ground motion excitation of the Northridge record, restraining drift in pier-columns increases shear demand to a peak of 795.0 kips and generates larger bending forces distributed towards the base of the columns. The demand at the bottom of the columns reaches a peak moment demand of 5095.1 kip-ft, while the top of the columns induces a comparatively lower moment demand to the caisson case at 4159.83 kip-ft. Plastic hinges subsequently are developed across all eight piers; at the top locations of six piers and at the bottom of all eight piers locations.

In comparison with the caisson support case, plastic hinges are developed at the top and bottom of columns in the spread footing case, while the development of plastic hinges was limited to the top of the column in the caisson support case. A seismically designed caisson support may be beneficial to lowering moment demand across the substructure, and specifically reducing the concentrated bending forces at the bottoms of the pier columns.

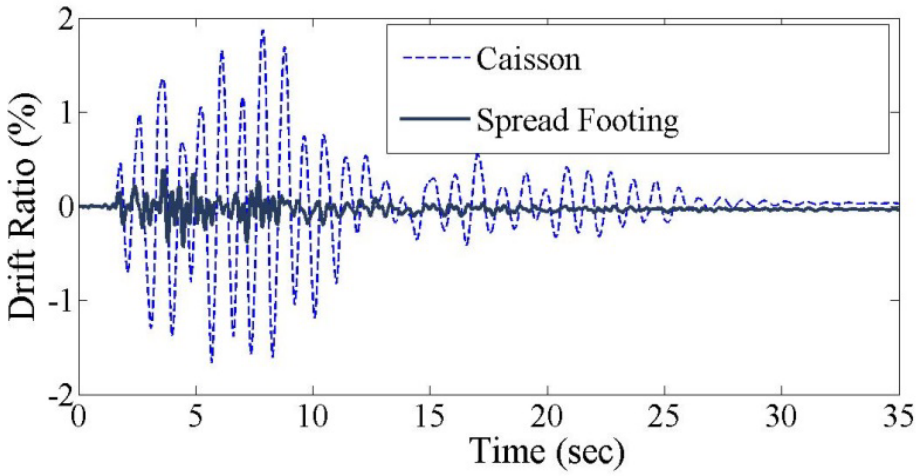

Figure 4.10 Drift Ratio of Pier-Column

Table 4.2 summarizes the bridge performance comparison subjected to different load exposures. The first exposure serves as baseline exposure, which includes dead load only. As compared with the dead load only scenario, much larger vertical displacement on the bridge deck is observed. Significantly larger column drift ratio, shear, and moments on both longitudinal and transverse directions are also observed. The third scenario is about the bridge under stochastic traffic load. Traffic load causes about 50% vertical displacement of that caused by seismic, but much less of other responses. The scenario of both seismic and traffic load shows little difference as compared with the seismic only scenario, which is different from what is observed for long-span bridges (e.g., Liu et al. 2010). It suggests that for short- or medium-span bridges like the one studied, the inclusion of traffic load along with seismic load does not control the bridge seismic design except for longitudinal moment on the top of the column. It is probably because of limited traffic on these particular short-span bridges and relatively rigid nature of the bridge. However, the prototype bridge is a typical two-span bridge with large bridge width. The trends of other types of short-span and medium-span bridges are not yet clear. Therefore, a general conclusion cannot be made before more comprehensive studies are conducted on different configurations.

Table 4.2 Summary of the Performance Subjected to Different Load Exposures

Exposure	Vertical Deck Disp (in.)	Drift Ratio Column (%)	Column Axial Load (kips)	Column Shear (kips)	Column Long. M –Top (kip -ft)	Column Transverse M. –Top (kip -ft)
Dead	0.87	0	766	0.4	2.1	33
Seismic	2.49	1.68	911	463	4103	618
Traffic	1.10	0.1	871	25	278	59
Traffic+Seismic	2.50	1.67	931	464	4113	616
Seismic+Scour (2.5 ft)	2.46	1.63	933	459	4167	611
Seismic+Traffic+Scour(2.5 ft)	2.48	1.62	915	457	4110	613
Seismic+Traffic+Scour(5.0 ft)	2.47	1.56	932	457	4115	610
Seismic - Vertical Ground Motion	2.50	1.62	945	464	4102	617
Seismic - Vertical +Traffic	2.51	1.62	952	464	4107	616
Spread Footing-Traffic +Seismic	2.01	0.41	864	716	3778	1090

Scour is found not to have a substantial effect on the bridge's response in this study. The results of the scenario with both scour and traffic along with seismic suggests that the combined effect of scour and traffic is not significant for this bridge. To realistically consider the presence of stochastic, traffic may slightly lower the bridge response when only scour and seismic are considered. Two different scour depths (2.5 ft. and 5 ft.) were studied separately. Most bridge responses with higher scour depth (5.0 ft.) are actually smaller than those with lower scour depth (2.5 ft.). This finding shows that the most critical scenario is not necessarily the one when there is more scour. It is known that different scour depths change not only the local properties of the column, but also the modal properties of the whole bridge and in turn the seismic excitation. Therefore, the combined effect of scour and earthquake, although showing a subtle difference in this example, exhibit complex characteristics deserving case-by-case study.

The inclusion of vertical ground earthquake excitation shows some slight increase of vertical bridge deck displacement but do not control most other responses. As discussed above, because the prototype bridge with caissons shows excessive bending forces, the alternative of a spread footing is also studied for comparison purposes. Not surprisingly, it is found that the bridge with spread footing exhibits a smaller column drift ratio, but increased column shear forces and transverse moment on the top of the column. Meanwhile, the longitudinal moment at the top of the column and the column axial load are both reduced.

Based on the results of comprehensive scenarios as listed in Table 4.2, it is found that the controlling cases for different bridge responses subjected to realistic service and extreme loads are quite complex. In the present study, after the analytical methodology is developed, a typical two-span bridge with medium span lengths is studied for various load cases. As the initial effort on numerically analyzing the bridge performance under multiple loads (hazards), no general conclusion should be made before a good number of different bridges with representative configurations are studied. Based on the results of this prototype bridge, the following observations are made.

1) This bridge is located in the Denver metro area where moderate-to-high traffic flow is expected most of the time. Although a substantial difference is not observed with the

inclusion of the traffic loads, the case with both seismic and traffic loads represents a more realistic scenario that could realistically occur. Although the substantiation is not significant, comparatively, the cases of “Traffic+Seismic” and “Seismic-Vertical+Traffic” control the vertical deck displacement, column axial load, column shear. The “seismic” case (i.e., with seismic only) controls drift ratio of column and transverse moment on the column top. Therefore, the inclusion of traffic load in the analysis not only represents more realistic situations on the bridge, but also may provide more critical demand and control the bridge design during seismic. The bridge performance subjected to joint seismic and traffic loads is much more complex than simply superposing the individual response. A bridge-specific study of seismic and traffic service load seems to be necessary.

2) In this example, the scour effect does not contribute substantial difference on bridge response. “Seismic+Scour (2.5 ft.)” controls longitudinal moment on the column top. With an increase in scour depth, the bridge response does not necessarily increase under seismic, which suggests complex nature, and no general observation can be made in regard to the contribution of scour effect on seismic response.

5. CONCLUSION AND FUTURE WORKS

This project was aimed at developing a general analytical methodology of structural performance of a typical short- and medium-span bridge subjected to seismic, scour, and service traffic loads. This includes the detailed FEM modeling with SAP 2000 on both superstructure and substructure; stochastic traffic flow simulation and dynamic interaction analysis; and time-history analysis of the dynamic components. By selecting a typical bridge in mountainous states, site-specific seismic analysis was conducted for different load scenarios. Some observations were made by comparing the results of different cases.

As the first step to investigate more realistic load scenarios, this study had several limitations due to the scope of the study. The limitations include (1) only one bridge and several configurations are studied; and (2) the study is limited to mountainous states with low to moderate seismic. As a result, some observations made in this study can disclose some initial findings specific to the specific bridge and seismic scenario. These findings shed some lights on the significance and direction of future studies. However, the writers express caution about extending the specific findings to all other medium-span or short-span bridges before further studies are conducted. Some general findings that can bring attention to future research and bridge designs include: (1) the study showed that more realistic modeling of extreme and service load is important; and (2) the load combination scenarios may control bridge designs in some situations. More comprehensive study, however, is needed to draw general conclusions and be incorporated into any future design guidelines.

6. REFERENCES

ACI Committee 318. (2008). *Building Code Requirements for Structural Concrete (ACI 318-08) and Commentary.*

Alipour, A., B. Shafei, & M. Shinozuka (2011). Seismic Performance Assessment of Highway Bridges Under Scour Effects. *TRB 2011 Annual Meeting.*

American Association of State Highway and Transportation Officials (2009). *AASHTO Guide Specifications for LRFD Seismic Bridge Design.*

Cai, C.S. and S.R. Chen (2004).“Wind Hazard Mitigation of Long-span Bridges in Hurricanes,” *Journal of Sound and Vibration*, 274 (1-2), 421-432.

Chen, S. R. and C.S. Cai (2007). “Equivalent wheel load approach for slender cable-stayed bridge fatigue assessment under traffic and wind: Feasibility study.” *Journal of Bridge Engineering, ASCE,* 12(6), p. 755-764.

Chen, S.R. and J. Wu (2010). “Dynamic performance simulation of long-span bridge under combined loads of stochastic traffic and wind.” *Journal of Bridge Engineering*, 15(3), p. 219-230.

Chen, S.R. and J. Wu (2011). “Modeling stochastic live load for long-span bridge based on microscopic traffic flow simulation.” *Computer & Structures*, 89, p. 813-824.

Computers & Structures, Inc. (2010). *CSI Analysis Reference Manual.*

Crosti, C., M. Duthinh & E.F. Simiu (2011). “Risk Consistency and Synergy in Multihazard Design.” *Journal of Structural Engineering ASCE* , 844-849.

Duthinh, D., & E. Simiu (2009). “Safety of Structures in Strong Winds and Earthquakes: Multi-Hazard Considerations.” *Journal of Structural Engineering ASCE* .

FEMA (2004). *FEMA Report 424: Design Guide for Improving School Safety in Earthquakes, Floods, and High Winds.*

Green, M. & D. Cebon (1994). “Dynamic Response of Highway Bridges to Heavy Vehicle Loads: Theory and Experimental Validation.” *Journal of Sound and Vibration* , 51-78.

Hida, S.E. (2007). “Statistical Significance of Less Common Load Combinations.” *Journal of Bridge Engineering ASCE* , 389-393.

Kameda, H., Y. Murono, Y. Maekawa, and N. Sasaki (1992). Dynamic Structure-Vehicle Interaction for Seismic Load Evaluation of Highway Bridges. *Proceedings of the Tenth World Conference on Earthquake Engineering*, Madrid, Spain, July 19-24, pp. 4861-4866.

Kim, C., M. Kawatani, S. Konaka, & R. Kitaura (2011). “Seismic responses of a highway viaduct considering vehicles of design live load as dynamic system during moderate earthquakes.” *Structure and Infrastructure Engineering* , 523-534.

Kiremidjian, A., J. Moore, Y.Y. Fan, O. Yazlali, N. Basoz, & M. Williams (2007). “Seismic Risk Assessment of Transportation Network Systems.” *Journal of Earthquake Engineering* , 371-382.

Kozar, I. (2009). “Security aspects of vertical actions on bridge structure: Comparison of earthquake and vehicle induced dynamical forces.” *Engineering Computations: International Journal for Computer-Aided Engineering and Software* , 145-165.

Lee, W.K., & S.L. Billington (2011). “Performance-based earthquake engineering assessment of a self-centering, post-tensioned concrete bridge system.” *Earthquake Engineering and Structural Dynamics* , 887-902.

Liu, M.F., T.P. Chang, and D.Y. Zeng (2011). “The interactive vibration behavior in a suspension bridge system under moving vehicle loads and vertical seismic excitations.” *Applied Mathematical Modeling*, 35, 398-411.

Mackie, K., & B. Stojadinovic (2006). “Post-earthquake functionality of highway overpass bridges.” *Earthquake Engineering and Structural Dynamics* , 77-93.

Moehle, J., & G.G. Deierlein (2004). A Framework Methodology for Performance-Based Earthquake Engineering. *13th World Conference on Earthquake Engineering.* Vancouver, B.C., Canada.

Nagel, K., & M. Schreckenberg (1992). “A Cellular Automaton Model for Freeway Traffic.” *Journal of Physics, France* , 2221-2229.

Padgett, J.E. & R. DesRoches (2007). “Bridge Functionality Relationships for Improved Seismic Risk Assessment of Transportation Networks.” *Earthquake Spectra* , 115-130.

Potra, F.A. & E.F. Simiu (2009). “Optimization and Multihazard Structural Design.” *Journal of Engineering Mechanics ASCE* , 1472-1475.

Rickert, M., K. Nagel, M. Schreckenberg, & A. Latour (1996). “Two Lane Traffic Simulations Using Celluler Automata.” *Physica A* , 534-550.

Terzic, V. & B. Stojadinovic (2010). *PEER 2010/103: Post-Earthquake Traffic Capacity of Modern Bridges in California.*

Washington State Department of Transportation (2012). *WSDOT Bridge Design Manual M23-50./0.*